Solid State Phenomena
ISSN: 1662-9779, Vol. 387, pp 9-19
doi:10.4028/p-ZoJg4h

Submitted: 2025-12-18
Revised: 2026-02-10
Accepted: 2026-02-17
Online: 2026-04-14

Process Influences on Plastificate and Fiber Microstructure Formation: An LFT-D Compression Molding Parameter Study

Christoph Schelleis[1,a*], Luca Meckes[1,b] and Frank Henning[1,c]

[1]Fraunhofer Institute for Chemical Technology ICT, Joseph-von-Fraunhofer-Str. 7, 76327 Pfinztal, Germany

[a*]christoph.schelleis@ict.fraunhofer.de, [b]luca-meckes@web.de, [c]frank.henning@ict.fraunhofer.de

[a]christoph.schelleis@ict.fraunhofer.de [*]corresponding author

Keywords: FRTP, composites, processing, charge, plastificate, lofting, fiber content, fiber orientation.

Abstract. Direct compounding of long fiber thermoplastic (LFT-D) materials in compression molding are two complex processes in series linked by the plastificate. Continuous compounding and sequential compression create a time-dependent property progression along the extrusion direction of the plastificate. Under variation of secondary parameters, extruder die temperature, and die height of the LFT-D line, samples of plastificates, flow fronts and plates are manufactured and characterized. The plastificate density progression along the extrusion direction is primarily influenced by the temperature of the die. Lofting of the plastificate is higher at high temperatures while the density difference along the extrusion direction is lower. This density difference is known to influence fiber orientations and mechanical properties. The flow front of the material filling the mold is skewed because of the density difference. We show that the skewness is mainly influenced by the die height and is lower at high die heights. The fiber content distribution in the plate is discussed and found to be influenced by the length of the plastificate which is in turn determined by the secondary parameters. These secondary parameters of the LFT-D line can play a role in process optimization once the primary parameters are selected. This work provides clues and observations of principles for such optimizations.

Motivation and State of the Art

Earth's resources are finite and need to be spent only with great care [1]. Transportation of goods as well as personal mobility are pillars of wealth of our society, yet at the same time this sector accounts for roughly a quarter of the worlds CO_2 emissions [2]. A balance must be struck to conserve both the environment and society's wealth.

In vehicle manufacturing, identical parts are often used across model series and even brands [3]. These are an impactful lever for producing resource-saving components. With the proliferation of battery-powered aircraft, manned and unmanned aircraft, to be manufactured in similar quantities, the correct process description is becoming increasingly important. Long fiber reinforced thermoplastic (LFT) materials are a widely used material class in the automotive industry [4]. Polymer matrix and fibers, usually glass, are produced in various ways balancing processability and part performance [5]. Compression molding is an effective processing route with lower fiber attrition compared to injection molding [6]. The LFT-Direct (LFT-D) process has, since its inception more than two decades ago, pushed for ever higher market shares [7].

A processing scheme for LFT-D compression molding is given in Fig. 1. In a) two twin screw extruders (TSE) are, compounding the polymer melt from granulates and additives (TSE1), and gently incorporating the reinforcing fiber from continuous rovings (TSE2). A detailed description of the processing route is presented by Schelleis et al. [8], as are parameter studies [9] and selected mechanical properties [10,11]. At the end of TSE2 the plastificate or charge is cut to size and exits the LFT-D line to be compression molded immediately. The fibers in the plastificate are arranged in a spring-like double helix pattern [12–14] which relaxes as soon as the restrictions of the die are removed. This relaxation is called lofting [15] and will lead to an increase in porosity and conversely

a decrease in density [16]. The LFT-D compression molding process alternates from continuous compounding to discontinuous compression molding. This results in the plastificate having an old and a new end and a time gradient in between. Material will be sitting on a heated chain belt until enough material to fill the mold is produced. The material has an age in this process, and both ends of the plastificate can be referred to as old and new end (Fig. 1 a)). Once this amount has been extruded, the new end is formed. Accordingly, the relaxation lasts longest at the old end and the density of the plastificate ρ_{plast} is expected to be lowest here. Two conclusions can be drawn from this. First, the actual density does not equal the calculated density ρ_{calc} of the composite. Second, the center of volume does not coincide with the center of mass [17]. This is described in Fig. 1 a) with the actual length of the plastificate l_{plast} and the nominal length of the plastificate $l_{plast,calc}$ if it was pore-free. The pore-content decreases towards the new end, as was shown by Blarr [16]. The distance between the centers of mass and volume created by lofting is called D_l.

The plastificate is placed in the open mold and molded under high pressure, usually 200 bar [18]. Shown in Fig. 1 b) and c) is the side-aligned placement of the plastificate representing a distinct direction of flow (grey arrow). During the compression molding step, the distinct fiber microstructure of an LFT-D compression molding material is formed. A shell-core effect of perpendicularly aligned fiber orientations can be found in the charge area.

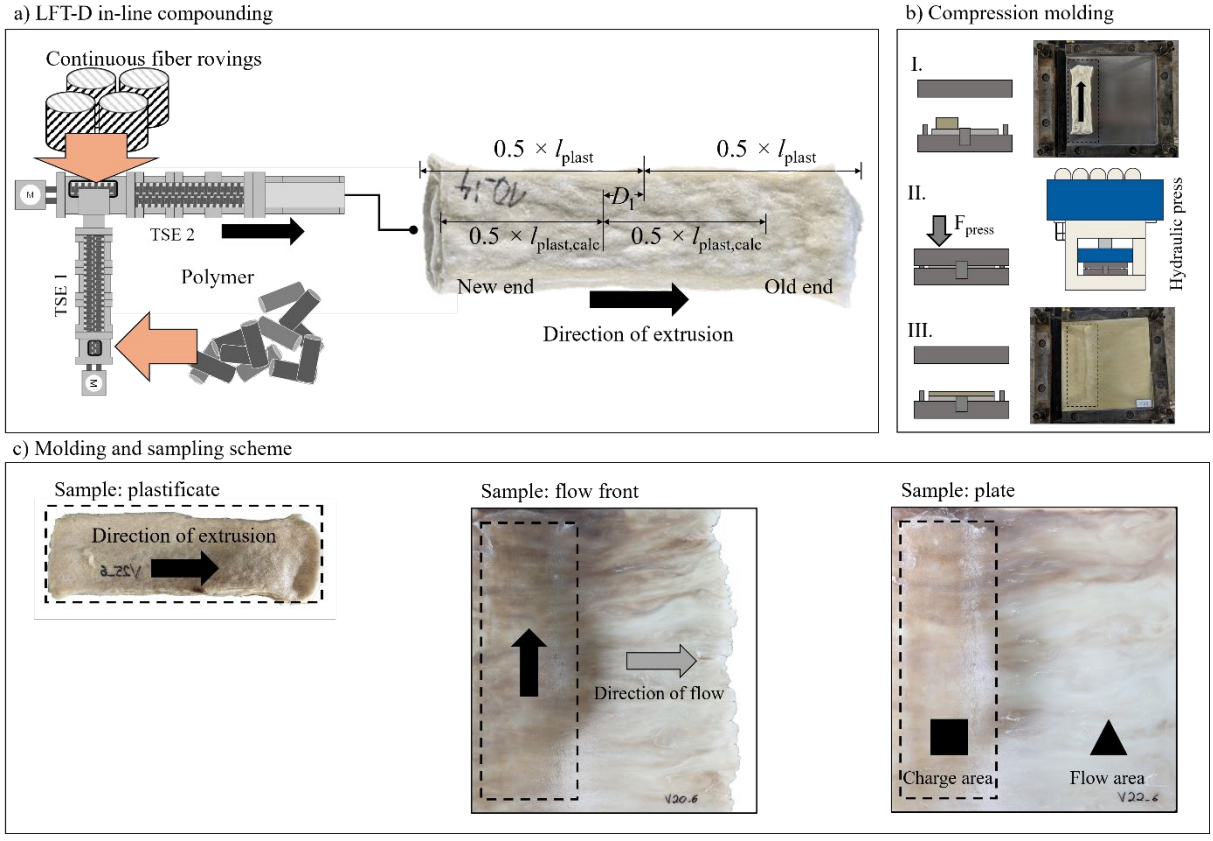

Fig. 1. Depiction of compounding a), compression molding b), and sampling c) schemes. Plastificate measurement terminology is given in a).

Microstructure.

The fiber microstructure defines the mechanical properties of the part [19]. A differentiation between charge and flow area (square and triangle in Fig. 1 c)) is regularly considered in the state of the art. Fiber mass content w_f is subject to shear-induced migration phenomena and does increase with flow path in the direction of flow (cf. grey arrow Fig. 1 c)) [20,21]. Deviations in fiber orientation as small as 10° can result in a significant drop in tensile properties [22]. The fiber orientation in LFT-D samples is often reported to be out of 0° alignment [23–25]. This was linked to a skewed flow front (cf. sample: flow front in Fig. 1 c)) caused by the distribution of density ρ_{plas} in the plastificate [26].

In fact, the density has a gradient ∇ρ from old to new end, being denser at the new end. This gradient is calculated according to Eq. 1 and stands for the density decrease along the length of the plastificate while correcting for different l_{plast}. It can be understood as an incline.

$$\nabla\rho = \Delta\rho / l_{plast}. \quad (1)$$

The plastificate does link both the compounding and compression molding processes. A discussion of the influence of the main LFT-D processing factors extruder screw speed, polymer throughput, and roving amount on the plastificate and further the flow front skewness s_{ff}, fiber orientation and w_f was presented by Schelleis [27].

Statement of Need and Approach

The process-microstructure relation must be described as accurately as possible and is essential for the precise simulation of the material [19,28,29]. In this work the die of TSE2 is the center of the investigation. The die has a fixed width but can be set to different heights and temperatures. An experimental plan is developed where and as well as the closing speed of the press are varied. Plastificates, flow fronts and square plates are produced and characterized (cf. Fig. 1 c for depictions of the samples). Quality criteria of the investigation are ρ_{plas} and ∇ρ, s_{ff} and w_f.

Materials, Processing and Methods

Material.

In this study a polyamide 6 material, Stabamid S22, with a matching masterbatch was provided by DOMO Chemicals. Glass fiber direct rovings JM StarRov895 were provided by Johns Manville Germany. The PA6 granulate was dried at 85 °C for 120 minutes immediately before processing.

Processing.

The materials were compounded on an LFT-D ILC line from Dieffenbacher, Eppingen, Germany. The die is 75 mm wide and set to h_{die} = 24 mm and h_{die} = 38 mm. The die temperature T_{die} is set to T_{die} = 265 °C and T_{die} = 280 °C. The primary LFT-D factors, extruder screw speed n_{TSE}, polymer throughput m_{pol} and roving amount n_{rov} are kept constant, so the throughput per hour $m_{LFT\text{-}D}$ as well as w_f are constant for all set points of the experiment. All relevant processing parameters are shown in Table 1. The time to produce the LFT-D amount needed to fill the mold $t_{LFT\text{-}D}$ is thus the same throughout the experiment. The length of the plastificate l_{plast} will change when the same amount of material is extruded through a die of smaller area. Selected plastificates are quenched in water for characterization immediately after the cut at the new end is made. Some plastificate are left to cool on their own to characterize the difference.

Table 1. Processing parameters of the LFT-D line and their set points for the experiments.

LFT-D production parameters		Set point	Resulting properties
primary	Extruder screw speed n_{TSE}	67.5 1/min	$m_{LFT\text{-}D}$ = 44.5 kg/h w_f = 33 %
	Polymer amount m_{pol}	30 kg/h	
	Roving amount n_{rov}	16 pcs.	
secondary	TSE2 temperature T_{TSE2}	280 °C	
	TSE2 die temperature T_{die}	265 °C or 280 °C	
	TSE2 die height h_{die}	24 mm or 38 mm	

Compression molding was done on a Dieffenbacher DYL 630 parallel guided, hydraulic press. Flow fronts and plates were molded in a 400 mm x 400 mm square mold heated to 80 °C (upper mold) and 85 °C (lower mold). Metal spacers were fixed to the mold for the fabrication of flow fronts, halting the molding process at a gap height of approximately 8 mm. The closing profile is given in Table 2. The closing speed towards the end of the compression molding process is a factor of the experiment

and changed from 5 mm/s to 10 mm/s. The closing speed is maintained for as long as the resistance of the material allows and the press switches to the force-profile. Molding is finished with 3200 kN (200 bar on the square mold). The difference between the profiles is visualized in Fig. 2 as a red curve (10 mm/s) and black curve (5 mm/s).

Table 2. Compression molding profile comprising position of the upper mold relative to the lower mold h_{mold} and closing speed of the upper mold v_{press}.

Gap height h_{mold} in mm	Closing speed v_{press} in mm/s
40	80
30	40
20	30
15	5 or 10
0	5 or 10

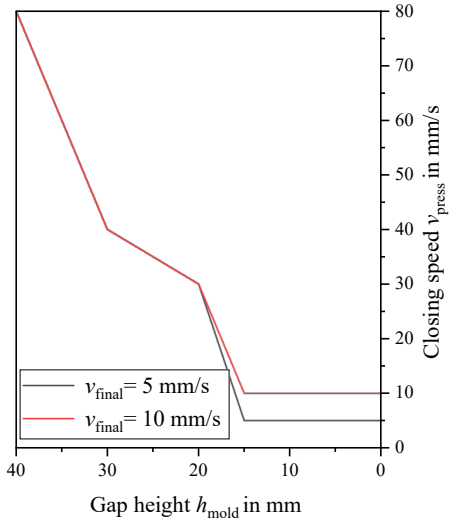

Fig. 2. Visualization of the press closing profile.

Methods.

Density characterizations of the plastificate were conducted by calculation after weighing and 3D scanning the volume [26,30]. The old and new ends are cut off at a length of 30 mm each as they are very rugged and difficult to scan. The density of these cut sections is not representative as the cut at the end of TSE2 staunches the plastificates. The rest is cut into four segments of the same length l_{seg} along the extrusion direction considering the time gradient. Preliminary investigations have shown that higher resolutions, for example eighths or sixteenths, do not provide any further insights [31]. The effective density of the entire plastificate ρ_{plast} is calculated as a mean value from all four segments. The density of the old end ρ_{old} has been calculated as a mean from the densities of the two older segments. The same approach was taken with ρ_{new} at the new end.

Flow fronts are photographed and analyzed. The flow-front skewness s_{ff} value is a representation of the mold being filled unevenly [26]. In Fig. 6 a scheme is given visualizing how to interpret s_{ff}. The flow front can be understood as a function that maps the flow progress over the extrusion length. This function has a minimum where the flow of the material has progressed the least. Here, a horizontal line can be drawn (solid red line in Fig. 6). The area, shown in grey in Fig. 6, between the function and the horizontal line has a center of area. Here, the s_{ff} value is a measure of the distance of the center of area to the mold middle (dashed black line in Fig. 6). To characterize the fiber migration, the plate is segmented into 80 mm squares that are burned off in an oven at 650 °C for 12 hours. The w_f is calculated from the mass of the polymer lost during this process. [20]

Results and Discussion

The results are presented in order of processing, starting with the plastificate, following with the flow fronts and ending with the plates. Unless stated otherwise a minimum number of five samples were taken to ensure sound statistics.

Plastificate.

Generally, the cut surfaces can be discussed. Two examples are shown in Fig. 3 a). Noticeably, the cut surface at h_{die} = 24 mm is coarse-pored than at h_{die} = 38 mm. Usual locations for big pores, shown in a), are between the two spiral impressions of the screw threads and on the outside. These pores

increase the volume, lower the density and are a source of uncertainty regarding the volume measurement [16]. In Fig. 3 b) the difference in l_{plast} resulting from the setting of h_{die} can be observed.

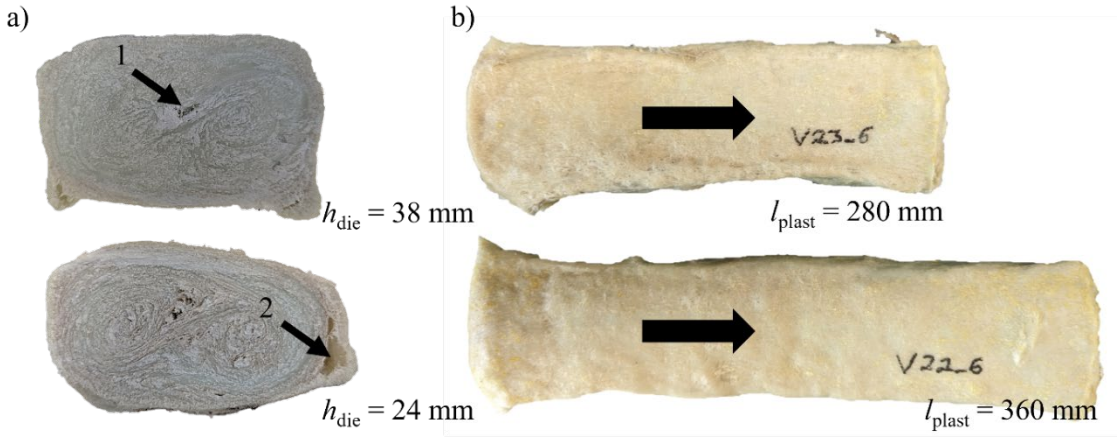

Fig. 3. Cut plastificate surface perpendicular to the extrusion direction a). Length comparison and results of ρ_{plast} measurement in relation to processing parameters T_{die} and h_{die} b).

The density measured across four segments is shown exemplary for two settings of h_{die} = 38 mm and h_{die} = 24 mm in Fig. 4. While plastificates vary individually (grey lines) a general trend can be seen once the measurements are averaged (red line). Once a linear fit function is drawn (dashed red line) the tendency is clear, density does decrease towards the old end. The ρ_{plast} at both the new and old ends is shown as a mean value of the densities of the first two and last two segments respectively. The density measurements show a high degree of deviation, especially the results of Fig. 4 b). The general tendencies of the density gradient or linear fit are valid, nonetheless. While the plastificates are quenched immediately after production a minimal amount of handling is required that can lead to changes in the shape and volume accordingly. Generally, at lower densities, the occurrence of big blisters below the shell layer of the plastificate can lead to a higher volume at lower weight and accordingly lower density.

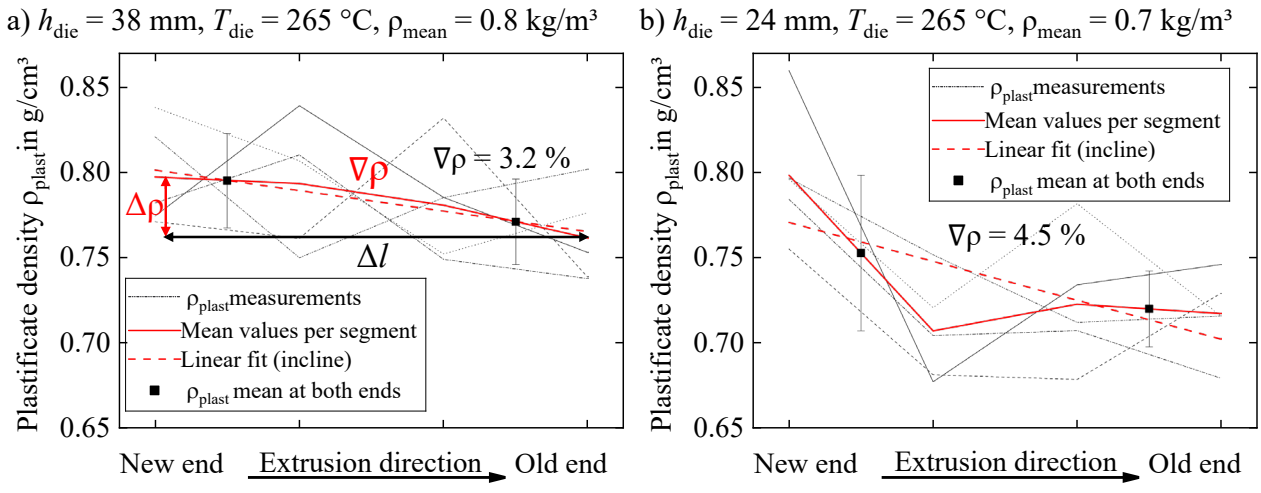

Fig. 4. Density measurements of four plastificate segments each for five plastificates along the extrusion direction for varied h_{die}.

The following Fig. 5 shows ρ_{plast} at the old and new end (checkered) of the plastificate for the parameter variation at the LFT-D line. The cut segments are indicated on the left. Both T_{die} and h_{die} are significant parameters influencing ρ_{plast} with h_{die} being the stronger influence (6.2 % difference in ρ_{plast}). Raising T_{die} from 265 °C to 280 °C lowers ρ_{plast} and rising h_{die} from 24 mm to 38 mm increases ρ_{plast}. Lofting can be understood as a relaxation of inner tensions in the plastificate as soon as the confines of the TSE2 die are gone. A colder surface of the plastificate will resist these forces and keep

the shape and volume closer to the dimensions of the die. The ∇ρ is higher at low T_{die} (blue columns) and slightly lower at higher h_{die}. The influence of T_{die} is stronger.

At w_f = 33 %, ρ_{calc} of the plastificate would be 1.4 g/cm³, implying a pore content around 45 % depending on choice of parameters. If ρ_{plast} is too low, processing can become difficult as needle grippers might lose the plastificate during handling. Also, material degradation is accelerated by a larger surface area as plastificates are open pored when lofting. A noticeable browning of plates can be observed.

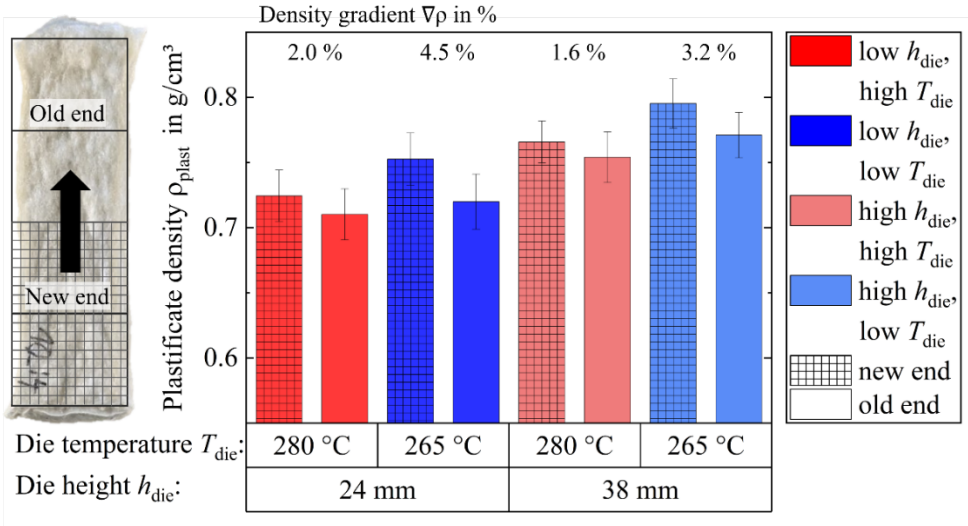

Fig. 5. Results of ρ_{plast} measurement in relation to processing parameters T_{die} and h_{die}. A plastificate with overlayed segments at old and new end is shown on the left.

Flow front.

Influences of h_{die}, T_{die} and v_{press} on s_{ff} are shown in Fig. 6. A photo of a flow front is shown on the left. The greyed area above the red line is noticeably skewed from the mold middle towards the new end of the plastificate (dashed charge area). The s_{ff} value does fluctuate, resulting in a big standard error and considerable coefficient of variation (CV) between 16.5 % and 83.3 %. A larger die height does consequently decrease the mean s_{ff} (arrows). A s_{ff} = 0 would mean that the material is distributed evenly left and right of the mold middle. The other parameters T_{die} and v_{press} are not significant, while step patterns can be seen nonetheless. The s_{ff} does greatly depend on ∇ρ which is also influenced by the factors so an excluding interaction must be considered. Noticeably, the lowest and highest s_{ff} are found at T_{die} = 280 °C. The influence of v_{press} is higher at T_{die} = 280 °C.

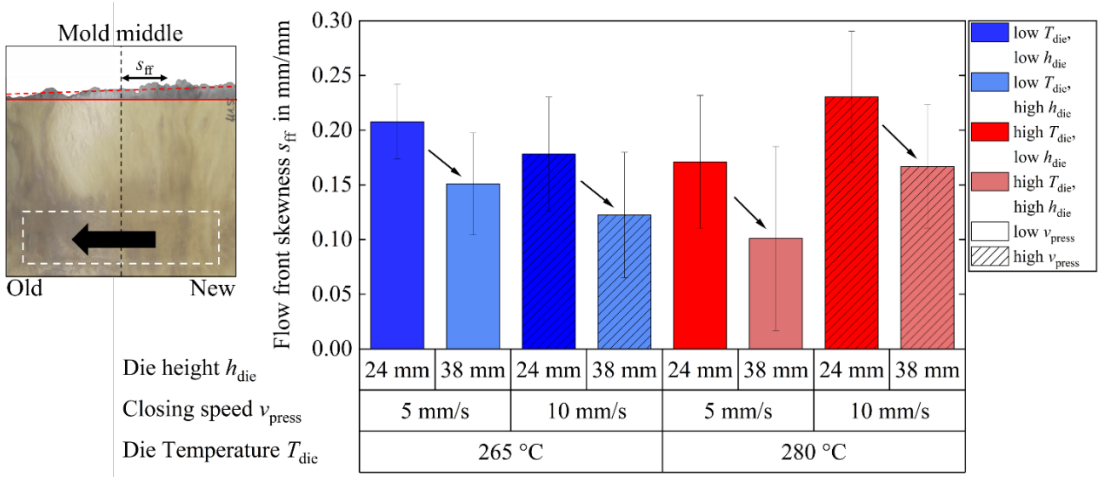

Fig. 6. The influence of h_{die}, T_{die} and v_{press} on s_{ff}. The relation of s_{ff} to the old and new plastificate ends in shown on the left.

Plate.

Fig. 7 features w_f for each of the twenty-five 80 mm by 80 mm segments of a plate. The difference is h_{die} and resulting from that, l_{plast}. The size of the charge area is noticeably larger for h_{die} = 24 mm shown as a white frame in Fig. 7 a). The fiber-matrix-separation starts as soon as the material starts flowing. The outer areas of the flow freeze on the cold mold wall. The closing mold gap pushes the LFT-D material into the remaining mold cavity. Shear between the static, frozen, material at the mold walls and the accelerating material in the center leads to migration of fiber in the polymer suspension [20,21]. Thus, w_f is higher outside the white frames marking the initial charge position. While $w_{f,mean}$ across the entire plate is the same for h_{die} = 24 mm and h_{die} = 38 mm the CV is higher for h_{die} = 24 mm when calculated from all segments. The plate is segmented into zones of mean fiber content in charge area $w_{f,C}$, and flow area $w_{f,F}$, by red-dashed lines. The change in w_f across the flow length from charge to flow is greater at h_{die} = 24 mm. Here, there is a difference of 7.1 %*pt*. while it is only 5.5 %*pt*. at h_{die} = 38 mm.

The density gradient as well as the position of the old and new end does not seem to play a role here. The choice of plastificate length through various parameters at the LFT-D line will influence the fiber microstructure in flow direction as well as perpendicular to the flow direction in the charge area (Fig. 7 b)).

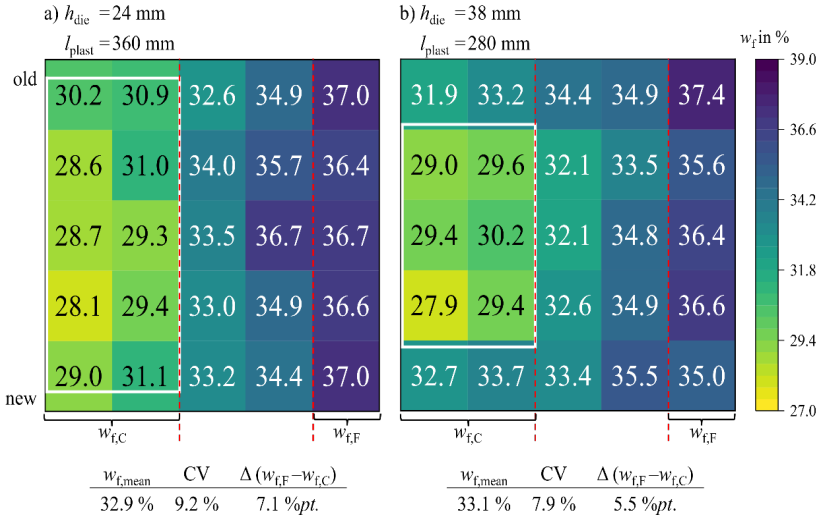

Fig. 7. Segment-wise distribution of w_f for low a) and high b) h_{die}.

Processing Recommendations

Following Fig. 8 is an attempt to visualize the mechanisms behind ∇ρ and processing influences in regards to lofting. The x-axis marks the extrusion time. At t_{end} the material for one plate is extruded, the plastificate is cut and molded directly. The plastificate is shown on top of the graph with the segments extruded continuously from t_{old} to t_{end}. Lofting starts for every segment once it is extruded, this point in time is for example t_{old} for the oldest segment. Note the extrusion direction from right to left (black arrow). Lofting can be seen as a function describing the decrease in density influenced by time t, T_{die} and h_{die} (as well as other factors not discussed here like n_{TSE} [27]). The shape of this function is assumed to be the same for all segments processed at the same set of parameters only influenced by parameter change. The shape of this function is based on observations that lofting starts and subsides quickly because the tension of the fiber decreases and the outer layer cools down. It is neither a continuous nor linear process. When plastificates are left to cool down uninterrupted the density gradient disappears as all segments loft to a similar extent.

Now considering two segments at the old and new end of the plastificate, this function can be drawn starting at different t_i during extrusion of a plastificate. For every segment, and every sub-segment and so on, the lofting starts at different t_i. The resulting density gradient ∇ρ can be seen at the time t_{end} where the plastificate is quenched or molded.

The influence of T_{die} and h_{die} on the shape of the function is shown in Fig. 8 b). Temperature stretches or staunches the curve in x-direction, the plastificate decreases its density quicker at higher T_{die} (red arrow in b)) This is shown in Fig. 5 where ρ is lower for higher T_{die}. The final extent of lofting is influenced by h_{die} mainly where the plastificate, if left to cool on air alone, will have a lower density at a low h_{die} (yellow arrow in b)).

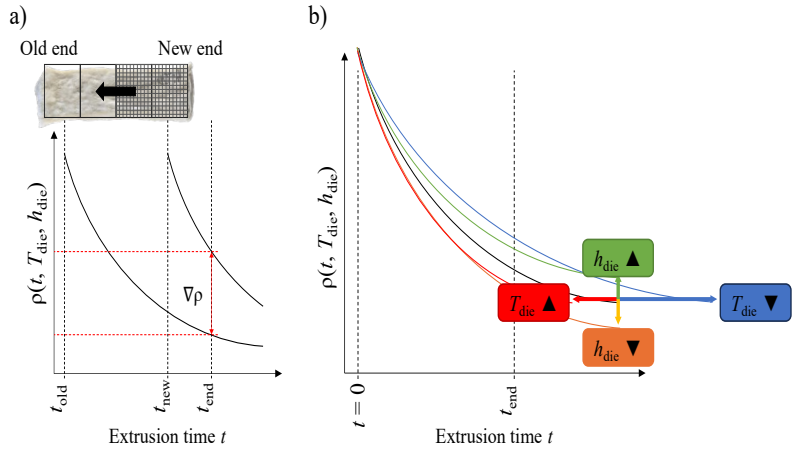

Fig. 8. Schematic explanation of ∇ρ between two functions a). Influencing factors on function shape from the experimental b).

The following Fig. 9 is an attempt to serve as a quick reference when dealing with a lofting related challenge in LFT-D compression molding. It is plausible, that ∇ρ depends on both factors h_{die} and T_{die} interacting in a way that leads to the results presented in Fig. 5 and Fig. 6. Parameter pairings from h_{die} and T_{die} can be chosen in the first column, the color coding is coherent to Fig. 8 where the influence on the ρ function is explained. Two things need to be considered. The extent of lofting and ∇ρ are not dependent on each other. A plastificate can be lofted a lot while not having a big ∇ρ. The combination of a larger die height, high h_{die}, and high T_{die} will lead to low lofting but quickly. The densities of the segments are at their final value quickly. This means, that when the plastificate is cut, the density of the first and last segments are very similar and ∇ρ is small (Fig. 9 a)).

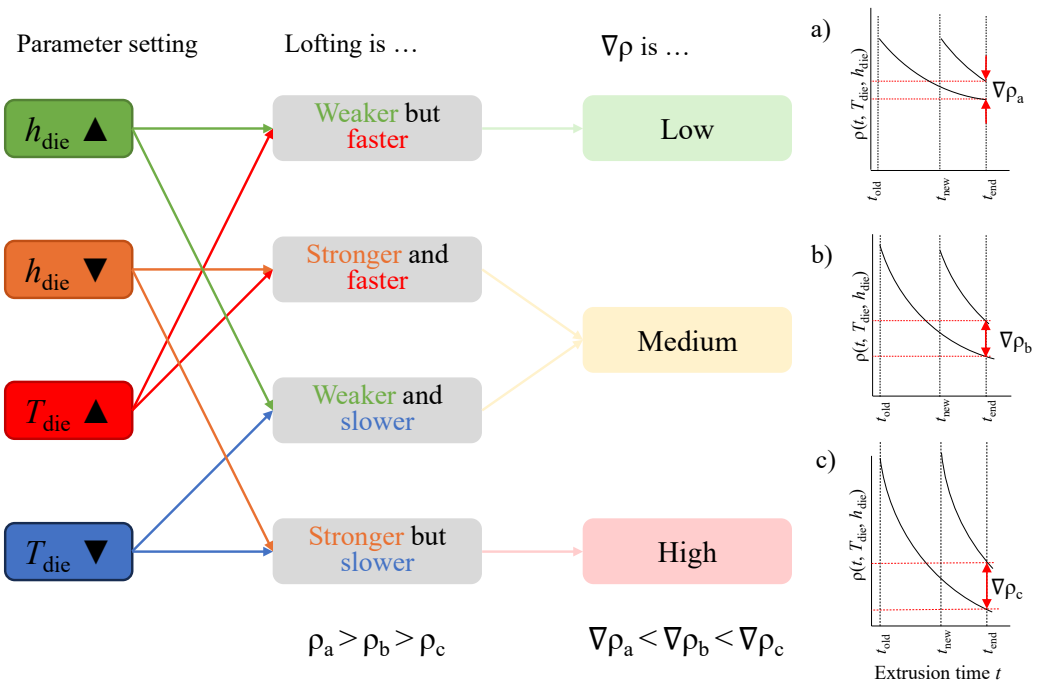

Fig. 9. Visualized influence of parameter settings on lofting and density gradient.

Summary

It was established, that the density of LFT-D plastificates does decrease with extrusion time towards its old end that has been out of the extruder the longest [30,31]. The pore content does increase in turn [16]. The spread of measured density and the difference between the old and new end is influenced by processing parameters especially the opening height of the extruder die and the temperature of the die (cf. Fig. 5). This uneven density distribution in the plastificate does influence mold filling and is known to influence the fiber orientations [26]. The plastificate length is highly influenced by the extruder die height and shown to impact the fiber content distribution across the plate (cf. Fig. 7) [20].

The plastificate is the crucial link between compounding and compression molding. It is directly influenced by the core factors of the LFT-D process such as screw speed, but also by secondary factors as demonstrated in this work. The plastificate does in turn influence important microstructure characteristics such as fiber orientation and fiber content. Further studies could investigate the influence of processing parameters on internal fiber orientation in the plastificate.

Acknowledgement

The initial research documented in this manuscript was funded by the Deutsche Forschungsgemeinschaft (DFG) (German Research Foundation), Project Number 255730231, within the International Research Training Group “Integrated engineering of continuous-discontinuous long fiber reinforced polymer structures” (GRK 2078).

The documentation and analysis of the results presented in this work was supported by the National Research Foundation of Korea (NRF) grant funded by the Korea government (MSIT) (RS-2024-00397400).

Support from DOMO Chemicals GmbH, as well as Johns Manville Europe GmbH in the form of trial materials is gratefully acknowledged.

References

[1] M. Wackernagel, N.B. Schulz, D. Deumling, A.C. Linares, M. Jenkins, V. Kapos, C. Monfreda, J. Loh, N. Myers, R. Norgaard, J. Randers, Tracking the ecological overshoot of the human economy, Proc. Natl. Acad. Sci. U. S. A. 99 (2002) 9266–9271. https://doi.org/10.1073/pnas.142033699.

[2] F. Henning, E. Moeller, Handbuch Leichtbau: Methoden, Werkstoffe, Fertigung, second Edition, Hanser, München, Wien, 2020.

[3] A. Kampker, H.H. Heimes, Elektromobilität: Grundlagen einer Fortschrittstechnologie, third Edition, Springer Vieweg, Berlin, Heidelberg, 2024.

[4] M. Schemme, LFT – development status and perspectives, Reinforced Plastics 52 (2008) 32–39. https://doi.org/10.1016/S0034-3617(08)70036-5.

[5] F. Henning, H. Ernst, R. Brüssel, LFTs for automotive applications, Reinforced Plastics 49 (2005) 24–33.

[6] T.A. Osswald, G. Menges, Materials science of polymers for engineers, third Edition, Hanser, Munich, Germany, 2012.

[7] E. Witten, V. Mathes, The European Market for Fibre-Reinforced Plastics and Composites 2022: Market developments, trends, challenges and outlook, AVK Market Report (2023).

[8] C. Schelleis, B.M. Scheuring, W.V. Liebig, A.N. Hrymak, F. Henning, Approaching Polycarbonate as an LFT-D Material: Processing and Mechanical Properties, Polymers (Basel) 15 (2023) 2041–2065. https://doi.org/10.3390/polym15092041.

[9] C. Schelleis, A. Hrymak, F. Henning, Optimizing processing parameters for glass fiber reinforced polycarbonate LFT-D composites, in: Proceedings of the SAMPE Europe Conference, Madrid, Spain, 2023.

[10] C. Schelleis, F. Henning, A. Hrymak, Comprehensive material development of glass fiber reinforced polyamide 6 LFT-D, in: Proceedings of ITHEC, Bremen, Germany, 2024, pp. 94–97.

[11] C. Schelleis, B.M. Scheuring, A. Hrymak, F. Henning, Study on mechanical characteristics of glass fiber-reinforced polycarbonate LFT-D for codico structures, in: Proceedings of the 23rd ICCM, Belfast, UK, 2023.

[12] K. Brast, Verarbeitung von langfaserverstärkten Thermoplasten im direkten Plastifizier-/ Pressverfahren. Dissertation (in german), Aachen, Germany, 2001.

[13] L. Schreyer, J. Blarr, K. Höger, N. Meyer, L. Kärger, Generation of Initial Fiber Orientation States for Long Fiber Reinforced Thermoplastic Compression Molding Simulation, in: Proceedings of the 20th ECCM, Lausanne, Switzerland, 2022.

[14] C. Perez, T. Osswald, S. Goris, Study on the fiber properties of a LFT strand, in: Proceedings of the 13th Annual SPE ACCE, Novi, MI, USA, 2013, pp. 1115–1126.

[15] F. Truckenmüller, H.-G. Fritz, Injection molding of long fiber-reinforced thermoplastics: A comparison of extruded and pultruded materials with direct addition of roving strands, Polymer Engineering & Science 31 (1991) 1316–1329. https://doi.org/10.1002/pen.760311806.

[16] J. Blarr, Development of Computational, Image Processing and Deep Learning Methods for the Microstructure Characterization of Carbon Fiber Reinforced Polyamide 6 Based on CT Images, Karlsruher Institut für Technologie (KIT), 2024.

[17] B.M. Scheuring, N. Christ, J. Blarr, W.V. Liebig, J. Hohe, J. Montesano, K.A. Weidenmann, Experimental and homogenized orientation-dependent properties of hybrid long fiber-reinforced thermoplastics, International Journal of Mechanical Sciences 280 (2024) 109470–109488. https://doi.org/10.1016/j.ijmecsci.2024.109470.

[18] F. Henning, Verfahrensentwicklung für lang- und endlosglasfaserverstärkte thermoplastische Sandwich-Bauteile mit geschlossenem Werkstoff-Kreislauf. Dissertation (in german), Fraunhofer-IRB-Verl., Stuttgart, Germany, 2001.

[19] U.N. Gandhi, S. Goris, T.A. Osswald, Y.-Y. Song, Discontinuous Fiber-Reinforced Composites: Fundamentals and applications, Hanser Publishers, Munich, Germany, 2020.

[20] C. Schelleis, L. Meckes, F. Henning, Fiber migration in compression molded LFT-D materials: characterization proposal and first results, in: Material Forming: ESAFORM 2025, Paestum, Italy, Materials Research Forum LLC, 2025, pp. 468–477.

[21] S. Goris, T.A. Osswald, Process-induced fiber matrix separation in long fiber-reinforced thermoplastics, Composites Part A: Applied Science and Manufacturing 105 (2018) 321–333. https://doi.org/10.1016/j.compositesa.2017.11.024.

[22] T. Osswald, Understanding Polymer Processing: Processes and Governing Equations, Hanser, Munich, Germany, 2018.

[23] B.M. Scheuring, Effect of hybridization in CoDico-FRTPs: Orientation-dependent characterization and analytical modeling in various climatic conditions. Dissertation, Karlsruhe, Germany, 2024.

[24] F. Garesci, S. Fliegener, Young's modulus prediction of long fiber reinforced thermoplastics, Composites Science and Technology 85 (2013) 142–147. https://doi.org/10.1016/j.compscitech.2013.06.009.

[25] J. Blarr, T. Sabiston, C. Krauß, J.K. Bauer, W.V. Liebig, K. Inal, K.A. Weidenmann, Implementation and comparison of algebraic and machine learning based tensor interpolation methods applied to fiber orientation tensor fields obtained from CT images, Computational Materials Science 228 (2023) 112286. https://doi.org/10.1016/j.commatsci.2023.112286.

[26] C. Schelleis, B.M. Scheuring, L. Schreyer, W.V. Liebig, A. Hrymak, L. Kärger, K.A. Weidenmann, F. Henning, Process-induced skewness of flow fronts and fiber orientations in LFT-D compression molding considering processing, characterization, and simulation, Journal of Thermoplastic Composite Materials 38 (2025) 2922–2944. https://doi.org/10.1177/08927057251344252.

[27] C.S. Schelleis, Characterization of Process Influences on Microstructure and Mechanical Properties of Long Glass Fiber Reinforced Polyamide 6 Plates in Compounding and Compression Molding. Dissertation, Karlsruher Institut für Technologie (KIT), Karlsruhe, Germany, 2025.

[28] F. Folgar, C.L. Tucker, Orientation Behavior of Fibers in Concentrated Suspensions, Journal of Reinforced Plastics and Composites 3 (1984) 98–119. https://doi.org/10.1177/073168448400300201.

[29] S. Tröster, Materialentwicklung und -charakterisierung für thermoplastische Faserverbundwerkstoffe im Direktverfahren. Dissertation (in german), Fraunhofer-IRB-Verl., Stuttgart, Germany, 2004.

[30] S. Löwe, Charakterisierung des Plastifikates an der Schnittstelle zwischen Compounding und Fließpressen langfaserverstärkter thermoplastischer Formmassen. Bachelor Thesis (in german), Karlsruhe, Germany, 2022.

[31] L. Meckes, Charakterisierung des LFT-D Plastifikates: Methodenentwicklung und Ermittlung der Prozesszusammenhänge mit Fokus auf die Dichteeigenschaften. Master Thesis (in german), Fraunhofer Society, Karlsruhe, Germany, 2024.